Design of Robust UPFC Based Damping Controller Using Biogeography Based Optimization

SA Al-Mawsawi*[1], A Haider[2], SA Al-Qallaf[3]
Department of Electrical and Electronics Engineering, College of Engineering, University of Bahrain
University of POB 32038, Sakheer, Bahrain
*Corresponding author, e-mail: aalmossawi@uob.edu.bh[1], aakabhar@uob.edu.bh[2],
saa1985@hotmail.com[3]

Abstract
        In this paper a new optimization algorithm, the biogeography based optimization (BBO) is employed to design a robust power oscillation damping (POD) controller using unified power flow controller (UPFC). The controller that is used to damp low frequency oscillation is designed over a wide range of operating points using two different objective functions. The obtained controllers are then verified through time-domain simulation over different loading conditions with different system uncertainties introduced.

Keywords: *Power system oscillation, unified power flow controller, Biogeography based optimization, multipoint optimization*

1. Introduction
        In the past few decades the power systems have witnessed a tremendous increase in size due to the rapid and continuous demand for power. This gave rise to the interconnection of power networks, thus increasing the systems complexity. This is due to the limited and restricted resources and the strict environmental constraints. The interconnection of remote power networks usually introduce low frequency oscillations in the range of 0.1~3.0Hz [1]. These oscillations can deteriorate the system performance if they are not sufficiently damped as they grow in magnitude, and finally lead to loss of synchronism [1, 2].
        This problem lead to use of power system stabilizers (PSS), are used to provide damping for generator oscillations. The PSS is a supplementary controller in the excitation systems. The PSS provides satisfactory operation under unusual or abnormal conditions which maybe encountered some times [1]. While PSS are effective in damping power oscillations, they suffer a drawback of being responsible of causing significant variations in voltage profile and they may even result in a leading power factor operation under sever disturbance conditions [3].
        On the other hand, FACTS controllers have come up as another solution for this problem. The flexiable AC transmission systems (FACTS) controllers were intended to solve various power system steady state control problems such as voltage regulation, power flow control, and transfer capability enhancement. The damping of the power system oscillations were introduced in FACTS as a supplementary control function [4]. Due to these capabilities, FACTS controllers' installation provides a better solution over PSS.
        Wang [5], has investigated the capabilities of Static Var Compensator (SVC), Controllable Series Compensator (CSC), and Phase Shifters (PS) to damp power system oscillations in an SMIB system. In [3], a coordinated control of PSS and SVC was introduced. Several references in literatures have investigated the capability of the Thyristor Controlled Series Capacitor (TCSC) to damp the power system oscillations through different approaches. In [6], a Genetic Algorithm (GA) based power system stabilizer using TCSC was designed.
        STATCOM capability to damp power system oscillations was superior to that of SVC [4]. In [7], a singular value decomposition (SVD) was introduced to investigate the controllability of poorly damped electromechanical modes via STATCOM input channels.
        Being the most versatile FACTS controller, UPFC had become an interesting field of research for damping power system oscillations. In [8], a UPFC based stabilizer was developed to mitigate torsional oscillations using shunt converter phase angle as a control signal. Abido et al [9], has introduced a particle swarm based stabilizer using UPFC in which he has investigated

the controllability of the UPFC different input channel to damp power system oscillations. It was observed that the shunt converter phase angle provides better controllability for damping electromechanical oscillations compared to the other input channels. In [2], a coordinated control design for UPFC and PSS based on particle swarm was developed.

In this paper, biogeography based optimization (BBO) algorithm is used to find the optimal parameters for the UPFC based damping controller. In order to find the optimal set of parameters to ensure the system robustness, the BBO searches for optimal sets of a time based objective function over a wide range of operating conditions. This time based objective function eliminates the need to linearize the system for finding the system eigenvalues. The time-based objective function for robust tuning is compared to the eigenvalue-based objective function for robust tuning of the controller.

2. System Modeling

2.1. Power System and Unified Power Flow Controller Model

Figure 1, shows a single machine infinite bus (SMIB) system with double transmission line circuits equipped with a UPFC. The UPFC consists of two three phase GTO based voltage source converters (VSC) connected back to back through a common DC link capacitor. The shunt converter or the excitation converter is coupled to the system through an excitation transformer (ET). The series converter or the boosting converter is coupled to the system through a boosting transformer (BT).
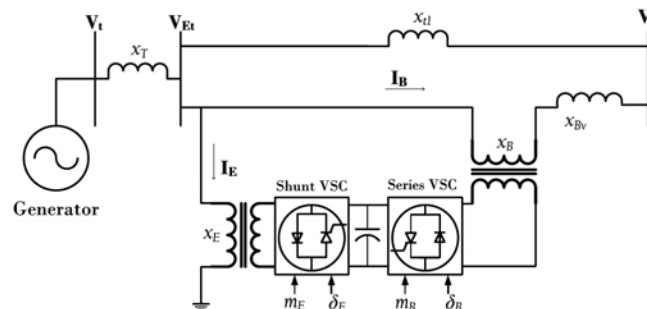
Figure 1. SMIB power system equipped with UPFC

By applying Park's transformation and by neglecting the resistances and transients of the excitation and boosting transformers the UPFC can be modeled as [5, 8, 9]:

$$\begin{vmatrix} v_{Etd} \\ v_{Etq} \end{vmatrix} = \begin{vmatrix} 0 & x_E \\ -x_E & 0 \end{vmatrix} \begin{vmatrix} i_{Etd} \\ i_{Etq} \end{vmatrix} + \frac{m_E v_{dc}}{2} \begin{vmatrix} \cos \delta_E \\ \sin \delta_E \end{vmatrix} \tag{1}$$

$$\begin{vmatrix} v_{Btd} \\ v_{Btq} \end{vmatrix} = \begin{vmatrix} 0 & x_B \\ -x_B & 0 \end{vmatrix} \begin{vmatrix} i_{Bd} \\ i_{Bq} \end{vmatrix} + \frac{m_B v_{dc}}{2} \begin{vmatrix} \cos \delta_B \\ \sin \delta_B \end{vmatrix} \tag{2}$$

$$\frac{dv_{dc}}{dt} = \frac{3m_E}{4C_{dc}} |\cos \delta_E \quad \sin \delta_E| + \frac{3m_B}{4C_{dc}} |\cos \delta_B \quad \sin \delta_B| \tag{3}$$

Where;
v_{Et} : Excitation transformer voltage
i_E : Excitation current
v_{Bt} : Boosting transformer voltage
i_B : Boosting current
C_{dc} : DC link capacitance
v_{dc} : DC link voltage

The UPFC has four control input signals where m_E and δ_E are the excitation branch amplitude and phase angles respectively, and m_B and δ_B are the boosting branch amplitude and phase angle respectively.

The nonlinear model of the generator shown in Figure 1 is given as:

$$\frac{d\delta}{dt} = \omega_B(\omega - 1) \tag{4}$$

$$\frac{d\omega}{dt} = \frac{1}{M}(-D(\omega - 1) + P_m - P_e) \tag{5}$$

$$\frac{dE'_q}{dt} = \frac{1}{T'_{d0}}\left(-E'_q + E_{fd} - (x_d - x'_d)i_d\right) \tag{6}$$

$$\frac{dE_{fd}}{dt} = \frac{1}{T_A}\left(-E_{fd} + K_A(V_{ref} - V_t)\right) \tag{7}$$

Where;

$P_e = v_d i_d + v_q i_q, v_q = E'_q - x'_d i_d, v_d = x_q i_q, V_t = \sqrt{(v_d^2 + v_q^2)},$

$i_d = i_{TLd} + i_{Ed} + i_{Bd},$ and $i_q = i_{TLq} + i_{Eq} + i_{Bq}$

From the above equations, the network currents can be rewritten as:

$$i_{TLd} = \frac{1}{x_{t1}}\left(x_E i_{Ed} + \frac{m_E v_{dc}}{2}\sin\delta_E - V_b \cos\delta\right) \tag{8}$$

$$i_{TLq} = \frac{1}{x_{t1}}\left(x_E i_{Eq} - \frac{m_E v_{dc}}{2}\cos\delta_E - V_b \sin\delta\right) \tag{9}$$

$$i_{Ed} = \frac{x_{BB}}{x_{d2}}E'_q + x_{d7}\frac{m_B v_{dc}}{2}\sin\delta_B + x_{d5}V_b \cos\delta + x_{d6}\frac{m_E v_{dc}}{2}\sin\delta_E \tag{10}$$

$$i_{Ed} = x_{q7}\frac{m_B v_{dc}}{2}\cos\delta_B + x_{q5}V_b \sin\delta + x_{q6}\frac{m_E v_{dc}}{2}\cos\delta_E \tag{11}$$

$$i_{Bd} = \frac{x_E}{x_{d2}}E'_q - \frac{x_{d1}}{x_{d2}}\frac{m_B v_{dc}}{2}\sin\delta_B + x_{d3}V_b \cos\delta + x_{d4}\frac{m_E v_{dc}}{2}\sin\delta_E \tag{12}$$

$$i_{Bq} = \frac{x_{q1}}{x_{q2}}\frac{m_B v_{dc}}{2}\cos\delta_B + x_{q3}V_b \sin\delta + x_{q4}\frac{m_E v_{dc}}{2}\cos\delta_E \tag{13}$$

where x_E and x_B represents the leakage reactances of ET and BT respectively, while x_{BB}, x_{d1}-x_{d7}, and x_{q1}-x_{q7} are given in [10].

2.2. System Linearized Model

In order to assess the stability of the system, and to construct an objective function based on the system eigenvalues, a linearized model of the system is to be determined. For this purpose, the system has to be linearized around different operating points. The linear model is given by:

$$\dot{x} = Ax + Bu \tag{14}$$

where x is the state vector and u is the input vector :

$$x = [\Delta\delta \quad \Delta\omega \quad \Delta E'_q \quad \Delta E_{fd} \quad \Delta v_{dc}] \tag{15}$$

$$u = [\Delta m_E \quad \Delta\delta_E \quad \Delta m_B \quad \Delta\delta_B] \tag{16}$$

where A and B are:

$$A = \begin{vmatrix} 0 & \omega_B & 0 & 0 & 0 \\ -\dfrac{K_1}{M} & -\dfrac{D}{M} & -\dfrac{K_2}{M} & 0 & -\dfrac{K_{pd}}{M} \\ -\dfrac{K_4}{T'_{d0}} & 0 & -\dfrac{K_3}{T'_{d0}} & \dfrac{1}{T'_{d0}} & -\dfrac{K_{qd}}{T'_{d0}} \\ -\dfrac{K_A K_5}{T_A} & 0 & -\dfrac{K_A K_6}{T_A} & -\dfrac{1}{T_A} & -\dfrac{K_A K_{vd}}{T_A} \\ K_7 & 0 & K_8 & 0 & K_9 \end{vmatrix} \qquad (17)$$

$$B = \begin{vmatrix} 0 & 0 & 0 & 0 \\ -\dfrac{K_{pe}}{M} & -\dfrac{K_{p\delta e}}{M} & -\dfrac{K_{pb}}{M} & -\dfrac{K_{p\delta b}}{M} \\ -\dfrac{K_{qe}}{T'_{d0}} & -\dfrac{K_{q\delta e}}{T'_{d0}} & -\dfrac{K_{qb}}{T'_{d0}} & -\dfrac{K_{q\delta b}}{T'_{d0}} \\ -\dfrac{K_A K_{ve}}{T_A} & -\dfrac{K_A K_{v\delta e}}{T_A} & -\dfrac{K_A K_{vb}}{T_A} & -\dfrac{K_A K_{v\delta b}}{T_A} \\ K_{ce} & K_{c\delta e} & K_{cb} & K_{c\delta b} \end{vmatrix} \qquad (18)$$

Where; K_1-K_9, K_{pu}, K_{qu}, and K_{cu} are the linearization constants.

2.3. UPFC-Based Damping Controller
The structure of the damping controller is shown in
Figure 2. It consists of a washout circuit which is provided to eliminate the steady state bias from the output of the damping controller.
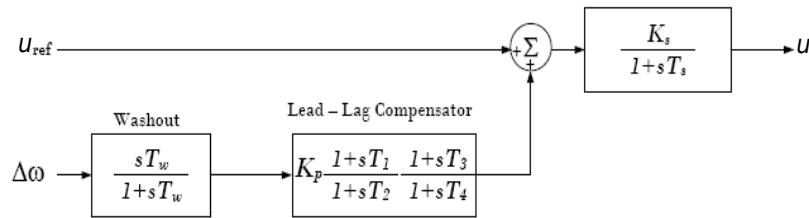
Figure 2. UPFC Based Damping Controller

A common practice for the design of the dynamic compensator is the use of a two stage lead-lag stage compensator. The two stage controller is also widely used for FACTS based damping controllers. On the other hand, PID controllers, as dynamic compensator in power system stabilizers, have also been implemented in damping system oscillations. In [11], a PID controller design based on particle swarm optimization for a multimachine system was implemented. In this paper the two stage lead-lag compensator is used. The transfer function of the two stages controller is given by:

$$T(s) = K_P \frac{(1 + sT_1)(1 + sT_3)}{(1 + sT_2)(1 + sT_4)} \qquad (19)$$

The control signal u of the UPFC can be any of the input signals m_E, δ_E, m_B, or δ_B. Based on [2, 9, 10], a singular variable decomposition was applied to measure the controllability of the electromechanical (EM) mode, and it was found that δ_E had the best controllability measurement compared to the other UPFC control signals. Thus it is logical to consider δ_E as the control signal when designing a damping controller.

2.4. Objective Function

In order to find the optimal set of parameters of the damping controller using BBO, an objective function needs to be optimized. Several time domain based performance indices have been proposed in literatures, such as integral of time multiplied by the absolute value of error (ITAE) criterion. In other performance indices such as eigenvalue based functions, the parameters are tuned in stabilizing power systems. This section presents two objective functions that are used to design a robust damping controller.

2.4.1. Eigenvalue Based Objective Function

In this approach, the damping coefficients of the eigenvalues are to be maximized. Then the damping coefficient ζ_i of the *i-th* eigenvalue is defined through the following equation:

$$\zeta_i = -\frac{\alpha_i}{\sqrt{\alpha_i^2 + \beta_i^2}} \tag{20}$$

Where α_i and β_i are the real and imaginary parts of the dominant eigenvalue respectively. A well damped power system is said to have a damping for all eigenvalues greater than 5% [**Error! Reference source not found.**]. Thus, the objective of the optimization problem is to achieve a damping for all eigenvalues greater than 5% over the range of the operating points.

Let Ξ_p be a vector of the damping factors of all eigenvalues of the p-th operating point in the set, where p=1,2,..,n for n operating points. Then the objective function to be maximized is:

$$\max J_e \tag{21}$$

Where; $J_e = min\left(min(\Xi_p)\right)$

2.4.2. Time Based Objective Function

For a robust tuning using the ITAE criterion, the objective function for set of operating points is designed as:

$$J_t = \sum_{i=1}^{p} \left(\int t|\Delta\omega_i|\, dt \right) \tag{22}$$

In both cases, the eigenvalue based objective function is to be maximized, while the time based objective function is to be minimized. The objective functions are subject to the following constraints:

$$
\begin{aligned}
K_{pmin} &\leq K_p \leq K_{pmax} \\
T_{1min} &\leq T_1 \leq T_{1max} \\
T_{2min} &\leq T_2 \leq T_{2max} \\
T_{3min} &\leq T_3 \leq T_{3max} \\
T_{4min} &\leq T_4 \leq T_{4max}
\end{aligned} \tag{23}
$$

In both cases only a DC voltage regulator is incorporated in the system in order to stabilize the DC link voltage. The parameters for the DC regulator are obtained beforehand and kept constant during the optimization process.

3. Biogeography Based Optimization

Biogeography-Based Optimization (BBO), introduced by Simon [**Error! Reference source not found.**] is a population based stochastic based evolutionary algorithm. Based on island biogeography theory, biogeography is the nature way to achieve optimal condition of life through the distribution of species among islands. This can be translated to a mathematical optimization problem, in which a number of candidate solutions referred to as population and each solution from the population is termed as individual. An individual that performs well on the objective function is analogous to an island that attracts different spices and it is said to have

high suitability index (HSI), and the individuals that perform poor on the objective function are analogous to low HSI islands where it attracts lower number of species.

The mathematical model of biogeography describes the immigration and emigration of species from an island. Islands with high HSI have high emigration rates and low immigration rates, due to the high population of species in that island. Low HSI islands have low emigration rates and high immigration rates and that is due to the large space and low species in these islands. The factors that characterize the HSI of an island are called suitability index variables (SIV), and it includes vegetative diversity, rain fall, topographic diversity, land area and temperature.

If an optimization problem was to be solved using BBO, the independent variables of the problem are analogues to the SIV of an island, and the solutions for that proposed individual is the HSI of such an island. As in biogeography theory that high HSI islands having lower immigration rate thus it will be more reluctant to change than the low HSI islands having immigration rates. Therefore, a good individual will have low tendency to change than poor individuals. On the other hand, the high HSI islands have high emigration rate and hence tendency to share its features with the low HSI islands having low emigration rates. Thus, the good individuals will share its features with the poor individuals. The addition of new features to poor individuals may raise the quality of those individuals.

MacArthur and Wilson [14], has illustrated the model of species abundance on a single island as shown in Figure 3. Immigration rate λ and emigration rate μ are functions of the number of species in the island.
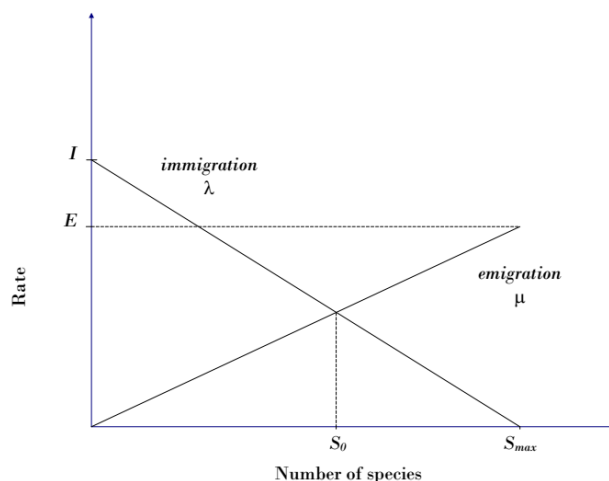
Figure 3. Species migration model of an island, based on [MacArthur and Wilson, 1967 [*Error! Reference source not found.*]]

In BBO each individual is represented by an identical species count curve with *E=I* for simplicity, as illustrated in Figure 4. The migration model shown below is called a linear migration model where λ and μ are both linear functions of the cost.
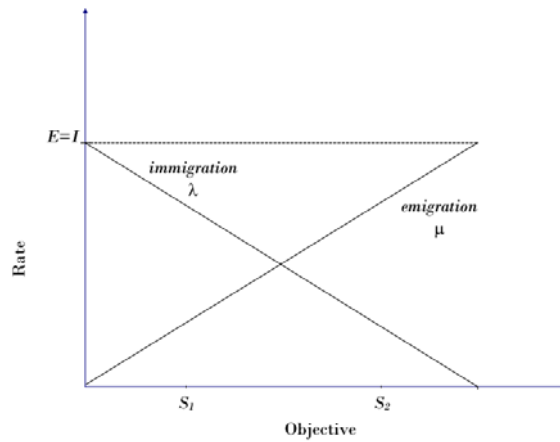
Figure 4. BBO individual species count curve with E=I

BBO has two major operations:

3.1. BBO Migration
Consider the following constrained optimization problem:

$$\min_{x \in \mathbb{R}^n} f(\mathbf{x}) \tag{24}$$

where $\mathbf{x} = [x_1, x_2, \cdots, x_n]$

x would be an individual which is analogous to an island, and $x_1, x_2, \ldots, x_n$ would be analogous to SIV of an island. Hence when a migration occurs the SIV's of an island will either immigrate to the individual or the will emigrate from the individual. In BBO a use of migration rates of each individual to probabilistically share information between individuals. There are different ways to implement migration in BBO, but in this study the original BBO developed in [**Error! Reference source not found.**] will be used which is referred to as partial immigration based.

Suppose that there are a population of size N and that x_k is the *k-th* individual in the population where $k \in [1, N]$, and the size of the optimization problem is n. $x_k(s)$ is the *s-th* independent variable in the individual, where $s \in [1, n]$. Based on the cost function evaluation the immigration probability λ_k, is given for the *k-th* individual and for all of its solution features $s \in [1, n]$, so in each generation there would be a probability of λ_k that this individual will be replaced.

Once a solution feature is selected to be replaced, then selection of the emigrating solution feature is done based on the emigrating probability of that individual $\{\mu_i\}$.

3.2. BBO Mutation
In BBO there are two main operators, i.e, migration and mutation. Simon [**Error! Reference source not found.**], has referred to mutation of SIV to be analogous to the introduction of an excursion to a habitat that will drive it away from its equilibrium point and that can happen randomly. An example is the arrival of large piece of flotsam to the island. Mutation rates are determined through the species count probabilities using equation (25).

$$\dot{P}_s = \begin{cases} -(\lambda_s + \mu_s)P_s + \mu_{s+1}P_{s+1}, & S = 0 \\ -(\lambda_s + \mu_s)P_s + \lambda_{s-1}P_{s-1} + \mu_{s+1}P_{s+1}, & 1 \leq S \leq S_{max} - 1 \\ -(\lambda_s + \mu_s)P_s + \lambda_{s-1}P_{s-1}, & S = S_{max} \end{cases} \tag{25}$$

From Figure 4, it can be seen that for low species count and high species count both have relatively low probabilities. While for medium species count they have high probabilities for change as they are near the equilibrium point.

The mutation rates can be found as:

$$m_i = m_{max}\left(1 - \frac{P_i}{P_{max}}\right)$$
(26)

Where;
m_i: the *i-th* individual mutation rate
m_{max}: the maximum mutation rate
P_i: *i-th* individual species count probability
P_{max}: Maximum species count probability from all individuals

4. Simulation Results

In this paper, the robust UPFC based damping controllers are tuned using BBO at 30 different loading conditions. The resulting controllers are tested for 4 different loading conditions with different parameters uncertainties that are presented in Table 1:

Table 1. System operating points and its uncertainties

Loading Condition	P_e	Q_e	System Parameter uncertainty
Light Loading	0.30	0.015	30% increase in line reactance x_{t1}
Nominal Loading	1.0	0.015	No parameter uncertainty
Heavy Loading	1.1	0.4	25% increase in machine inertia M
Leading power factor	0.7	-0.03	30% increase in field time constant T'_{d0}

By applying BBO for the two objective functions mentioned above, and by initializing the BBO for 100 generations, 100 individuals and for a maximum mutation rate of 0.005, the following results are obtained as shown in the Figure 5 and Figure 6. The figures below demonstrate the convergence curve of the objective functions. For Figure 5, as it was mentioned earlier, the objective is to maximize the damping ratio of the system where it reached (ζ_i=0.2496). As for the time based controller the objective was to minimize the absolute time error. It can be seen from the Figure 6, that the cost function has reached a value of 0.1247, i.e. $\sum_{i=1}^{p} ITAE_i = 0.1247$.
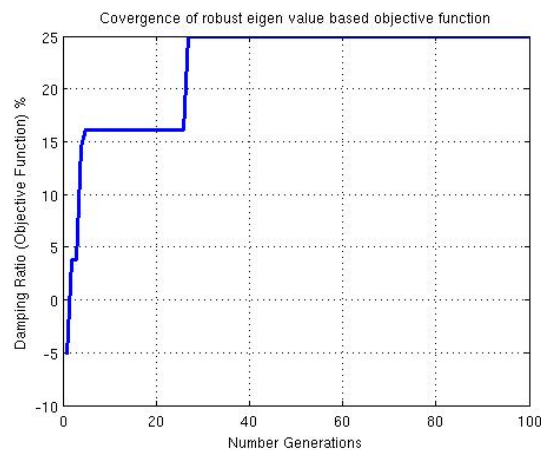
Figure 5. Convergence characteristic curve for a robust eigenvalue UPFC based damping controller using BBO
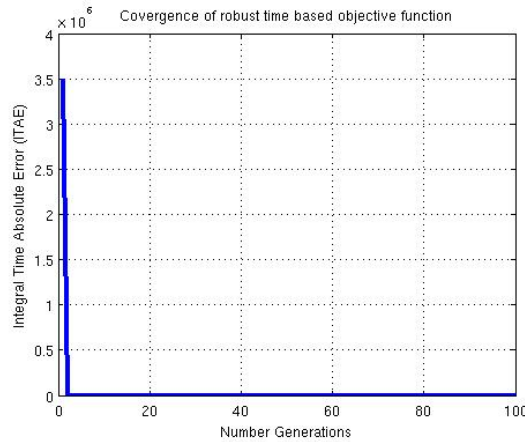
Figure 6. Convergence characteristic curve for a robust time-value UPFC based damping controller using BBO

The obtained parameters of the lead lag controller for the two objective functions are shown in

Table 2.

Table 2. Optimal parameter setting of the damping controller for the two objective functions

	Time-value based objective function	Eigenvalue based objective function
K_p	-94.8712	-95.7387
T_1	0.0143	0.0759
T_2	0.3284	0.7685
T_3	0.7778	1.4892
T_4	0.7126	0.5692

In order to analyze and compare the performance of the system using the resulting controllers, simulations were carried out for 10% step change in the mechanical power input P_m at the four different cases illustrated in Table 1. Table 3, shows the system eigenvalues for the two optimization approaches compared with the uncontrolled case. It can be shown that the system is stabilized for all the test cases.

Table 3. System eigenvalues for controlled and uncontrolled cases

	Light	Nominal	Heavy	Leading p.f
	-15	-15.7	-15.6	-16.8
No	-5.4	-4.8	-5.1	0.4 ± j3.5
Control	0.2±j3.3	0.6±j3.7	0.5± j3.6	-3.0
	-0.4995	-1.3	-0.8	-1.4
	-14.9	-15.7	-15.4	-16.8
	-6.2±j6.8	-6.6±j8.0	-6.9±j7.8	-6.9±j7.5
Eigen-value	-1.4±j3.9	-1.4±j4.2	-1.3±j4.0	-1.4±j4.3
Based	-6.1±j0.1	-5.4±j0.5	-5.3±j0.4	-4.5±j0.6
Control	-1.1	-1.1	-1.1	-1.1
	-0.02	-0.02	-0.02	-0.02
	-0.2	-0.2	-0.2	-0.2
	-15.2	-15.8	-15.6	-16.8
	-14.8	-14.6	-14.0	-14.4
	-1.9±j6.6	-1.8±j7.0	-2.4±j6.5	-1.8±j6.6
Time- value	-5.7	-5.2	-5.3	-3.9
Based Control	-2.0±j4.0	-2.2±j4.2	-1.9±j4.4	-2.4±j4.3
	-1.4	-1.4	-1.4	-1.4
	-0.02	-0.02	-0.02	-0.02
	-0.2	-0.2	-0.2	-0.2

4.1. Light Loading Condition
        Figure 7, shows the system response for 10% step change in mechanical input power under light loading conditions for the two designed damping controllers from the two approaches. It can be seen that the proposed time-value based tuned controller has greater overshoot compared with the eigenvalue based tuned controller which exhibits more damped response. Moreover, the settling time and the peak time are almost identical for both resulting controllers.
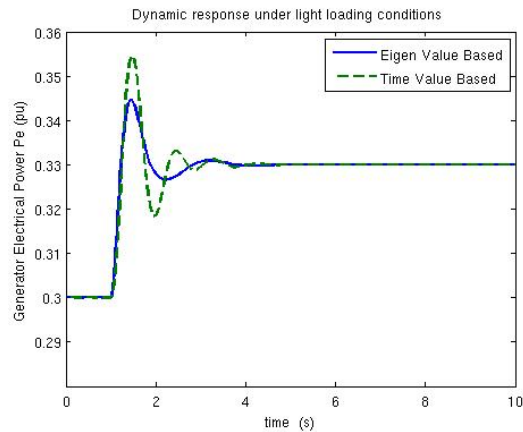
Figure 7: Dynamic response to a 10% increase in mechanical input power for light loading
condition: solid line eigenvalue based controller, dashed line time value based controller

4.2. Nominal Loading Condition
        The dynamic response of a nominal loaded generator for a 10% step change in P_m is illustrated in Figure 8. Similar to light loaded case the time-value based controller has an inferior response compared to the eigenvalue based controller in terms of the overshoot and damping.
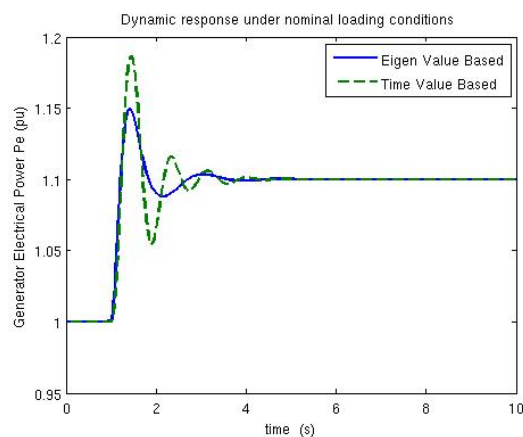
Figure 8. Dynamic response to a 10% increase in mechanical input power for nominal loading
condition: solid line eigenvalue based controller, dashed line time value based controller

4.3. Heavy Loading Condition

From Figure 9, even as the overshoot of the eigenvalue based controller is less compared to the time-based controller the settling time for both controllers is comparable under generator heavy loading conditions.
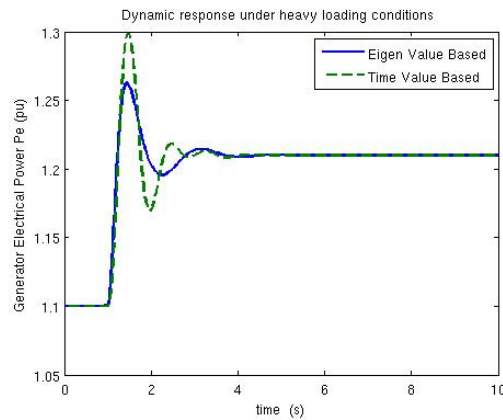
Figure 9. Dynamic response to a 10% increase in mechanical input power for heavy loading condition: solid line eigenvalue based controller, dashed line time value based controller

4.4. Leading Power Factor Condition

For a leading power factor loading condition of the generator, the response is shown in Figure 10 for the two controllers. Similar to the case above the time-value based controller is having a greater overshoot but a comparable settling time for the eigenvalue based controller.
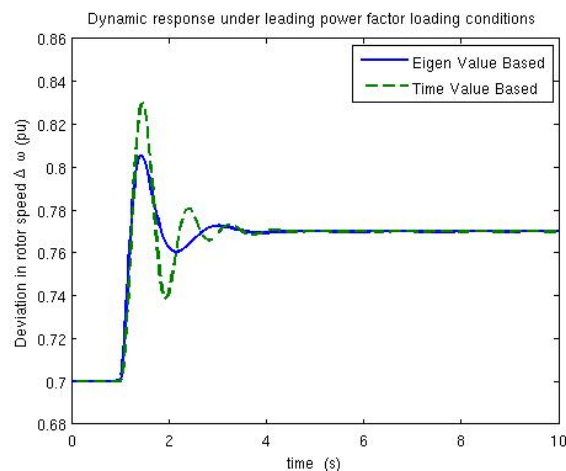
Figure 10. Dynamic response to a 10% increase in mechanical input power for leading power factor condition: solid line eigenvalue based controller, dashed line time value based controller

5. Conclusions

In this paper the biogeography based optimization (BBO) has been employed in designing a UPFC based damping controller. It also developed a new objective function to find the optimal parameters for damping controller, based on the integral time multiplied by the absolute error (ITAE) criterion. To test the effectiveness of the developed objective function, a comparison test was performed with the objective function based on the eigenvalue damping ratio, under four loading conditions and parameters uncertainties. It was shown that the effect of the objective function chosen for tuning the controller has a significant effect of the response

where the eigenvalue based objective function tuned controller yielded a better result than the developed objective function.

Appendix
Generator Data:
$x_d = 1; \ x_q = 0.3; \ x'_d = 0.3; \ D = 0; \ M = 10; \ T'_{d0} = 5.044; \ \omega_B = 100\pi \ rad/s; \ V_t = 1.05$
Transmission line:
$x_T = 0.1; \ x_{t1} = 0.6; x_{Bv} = 0.6$
UPFC:
$x_E = 0.1; \ x_B = 0.1; \ C_{dc} = 3; \ V_{dc} = 2;$
DC voltage regulator:
$k_{di} = -0.10; \ k_{dp} = -6.05$

References
[1]   K Padiyar. *Power system dynamics*. BS publications. 2008.
[2]   AT Al-Awami, MA Abido and YL Abdel-Magid. "Application of pso to design upfc-based stabilizers".
[3]   A Rahim and S Nassimi. "Synchronous generator damping enhancement through coordinated control of exciter and svc". *IEE Proceedings-Generation, Transmission and Distribution*. 1996; 143(2): 211–218.
[4]   M Abido. "Power system stability enhancement using facts controllers: A review". *Arabian Journal for Science & Engineering (Springer Science & Business Media BV)*. 2009; 34.
[5]   H Wang. "A unified model for the analysis of facts devices in damping power system oscillations. iii. unified power flow controller". *IEEE Transactions on Power Delivery.* 2000; 15(3): 978–983.
[6]   S Panda and NP Padhy. "Matlab/simulink based model of single-machine infinite-bus with tcsc for stability studies and tuning employing ga". *International Journal of Computer Science & Engineering*. 2007; 1(1).
[7]   M Abido. "Analysis and assessment of statcom-based damping stabilizers for power system stability enhancement". *Electric Power Systems Research*. 2005; 73(2): 177–185.
[8]   A Nabavi-Niaki and M Iravani. "Steady-state and dynamic models of unified power flow controller (upfc) for power system studies". *IEEE Transactions on Power Systems*. 1996; 11(4): 1937–1943.
[9]   MA Abido, A Al-Awami and Y Abdel-Magid. "Analysis and design of upfc damping stabilizers for power system stability enhancement". in *2006 IEEE International Symposium on Industrial Electronics.* 2006; 3: 2040–2045.
[10] M Abido, AT Al-Awami and Y Abdel-Magid. "Simultaneous design of damping controllers and internal controllers of a unified power flow controller". in *IEEE Power Engineering Society General Meeting*. 2006: 8.
[11] A Oonsivilai and B Marungsri. "Stability enhancement for multi-machine power system by optimal pid tuning of power system stabilizer using particle swarm optimization". *WSEAS transactions on power systems*. 2008; 3(6) 465–474.
[12] G Rogers. *Power system oscillations*. Kluwer Academic Boston. 2000.
[13] D Simon. "Biogeography-based optimization". *IEEE Transactions on Evolutionary Computation.* 2008; 12(6): 702–713.
[14] RH MacArthur. *The theory of island biogeography*. Princeton University Press. 1967; 1.